Synthesis and Characterization of Nanosized ZnS Confined in Ordered Mesoporous Silica

Wen-Hua Zhang,* Jian-Lin Shi, Hang-Rong Chen, Zi-Le Hua, and Dong-Sheng Yan

State Key Lab of High Performance Ceramics and Superfine Microstructure, Shanghai Institute of Ceramics, Chinese Academy of Sciences, 1295 Dingxi Road, Shanghai 200050, People's Republic of China

Received July 26, 2000. Revised Manuscript Received December 5, 2000

Nanosized ZnS has been prepared inside MCM-41 hosts by two related schemes, both of which are derived from surface modification methods. The ZnS-containing MCM-41 samples with and without the functional groups (ethylenediamine groups in this case) were designated as ZnS−ED−MCM-41 and ZnS−MCM-41(cal), respectively. The ZnS−MCM-41 composites were characterized by powder X-ray diffraction patterns, transmission electron microscopy, energy disperse spectra, N_2 adsorption−desorption isotherms, UV−vis diffuse reflectance spectra, and photoluminescence (PL) spectra. The ZnS was mainly formed and retained in the channels of the MCM-41 host, and its growth was controlled by the channels. In contrast, the amount of ZnS on the external surface is much smaller. The existence of ZnS inside the MCM-41 hosts resulted in a considerable decrease in surface area, pore diameter, and pore volume, and a massive blue shift in the UV−vis spectra was observed. In comparison with the ZnS−MCM-41(cal) sample, a dramatic increase in PL emission for the ZnS−ED−MCM-41 sample was observed, which was suggested to arise from a strong interaction between the ZnS clusters and the organic component. The nature of the PL spectra has been tentatively attributed to the sulfur vacancies in the present experiment. Finally, the synthesis of other sulfides, such as CdS and CuS clusters, has also been explored inside the channels of the MCM-41 host.

Introduction

In the past 2 decades, great efforts have been dedicated to the study of nanosized materials, which possess many novel properties that differ considerably from those of the bulk.[1] Because of the size quantization effects and potential applications in optoelectronics, low-dimensional semiconductor materials, including zero-dimensional quantum dots and one-dimensional quantum wires, have attracted special attention. Great advancement has been made in preparing nanostructured semiconductor materials in recent years;[2] for example, such materials have been prepared in colloids,[3] polymer matrixes,[4] self-assembled monolayers,[5] and zeolites.[6] Among these, to use porous materials as hosts for limiting the growth of clusters inside their pores is a relatively promising scheme. Several methods have been explored to fabricate such nanoclusters in the pores of zeolites, such as cation exchange[7] followed by in situ post-treatment and by the MOCVD method.[8] Copper nanoparticles and microsized fibers have been synthesized by using carbon nanotubes as the template.[9] In_2O_3[10] and silver[11] nanoparticles inside irregular mesoporous materials have also been prepared through incipient wetness impregnation of $In_2(SO_4)_3$ and $AgNO_3$, followed by thermal treatment.

Since the discovery of the novel mesoporous molecular sieves M41S in 1992,[12] much effort has been dedicated

* Present corresponding address: State Key Lab of Catalysis, Dalian Institute of Chemical Physics, Chinese Academy of Sciences, 457 Zhongshan Road, Dalian 116023, P. R. China.

(1) (a) Henglein, A. *Chem. Rev.* **1989**, *89*, 1861. (b) Ronsencher, E.; Fiore, A.; Vinter, B.; Berger, V.; Bois, P.; Nagle, J. *Science* **1996**, *271*, 168. (c) Yanagida, S.; Yooshiya, M.; Shiragami, T.; Pac, C.; Mori, H.; Fujita, H. *J. Phys. Chem.* **1990**, *94*, 3104.

(2) A special section of *Science* **1990**, *254*, 1300.

(3) (a) Spanhel, L.; Anderson, M. A. *J. Am. Chem. Soc.* **1991**, *113*, 2826. (b) Kamat, P. V.; Patrick, B. *J. Phys. Chem.* **1992**, *96*, 6829. (c) Henglein, A.; Giersig, M. *J. Phys. Chem. B* **1999**, *103*, 9533. (d) Wilcoxon, J. P.; Provencio, P. P. *J. Phys. Chem. B* **1999**, *103*, 9808.

(4) (a) Kane, R. S.; Cohen, R. E.; Silbey, R. *Chem. Mater.* **1996**, *8*, 1919. (b) Verelst, M.; Ely, T. O.; Amiens, C.; Snoeck, E.; Lecante, P.; Mosset, A.; Respaud, M.; Broto, J. M.; Chaudret, B. *Chem. Mater.* **1999**, *11*, 2702.

(5) (a) Colvin, V. L.; Goldstein, A. N.; Alivisatos, A. P. *J. Am. Chem. Soc.* **1992**, *114*, 5221. (b) Rizza, R.; Fitzmaurice, D.; Hearne, S.; Hughes, G.; Spoto, G.; Ciliberto, E.; Kerp, H.; Schropp, R. *Chem. Mater.* **1997**, *9*, 2969. (c) Hu, K.; Brust, M.; Bard, A. *Chem. Mater.* **1998**, *10*, 1160. (d) Sarathy, K. V.; Thomas, P. J.; Kulkarni, G. U.; Rao, C. N. R. *J. Phys. Chem. B* **1999**, *103*, 399.

(6) (a) Wang, Y.; Herron, N. *J. Phys. Chem.* **1987**, *91*, 257. (b) Herron, N.; Wang, Y.; Eddy, E. E.; Stucky, G. D.; Cox, G. D.; Moller, K.; Bein, T. *J. Am. Chem. Soc.* **1989**, *111*, 530. (c) Moller, K.; Eddy, M. M.; Stucky, G. D.; Herron, N.; Bein, T. *J. Am. Chem. Soc.* **1989**, *111*, 2561.

(7) (a) Uchida, H.; Ogata, T.; Yoneyama, H. *Chem. Phys. Lett.* **1990**, *173*, 103. (b) Liu, X.; Iu, K.-K.; Thomas, J. K. *Chem. Phys. Lett.* **1992**, *195*, 163.

(8) (a) MacDougall, J. E.; Eckert, H.; Stucky, G. D.; Herron, N.; Wang, Y.; Moller, K.; Bein, T.; Cox, D. *J. Am. Chem. Soc.* **1989**, *111*, 8007. (b) Steele, M. R.; MacDonald, P. M.; Ozin, G. A.; *J. Am. Chem. Soc.* **1993**, *115*, 7285. (c) Ozin, G. A.; Steele, M. R. *Adv. Mater.* **1994**, *6*, 300.

(9) Chen, P.; Wu, X.; Lin, J.; Tan, K. L. *J. Phys. Chem. B* **1999**, *103*, 4559.

(10) Zhou, H.; Cai, W.; Zhang, L. *Mater. Res. Bull.* **1999**, *34*, 845.

(11) Cai, W.; Tan, M.; Wang, G.; Zhang, L. *Appl. Phys. Lett.* **1996**, *69*, 2980.

10.1021/cm000621r CCC: $20.00
Published on Web 01/20/2001

to exploiting their formation mechanism,[13] surface modification,[14] and inclusion chemistry.[15,16] MCM-41 is a very attractive member in the M41S series due to its one-dimensional and hexagonal arrays of mesopores that can be adjusted within the range of 1.5−30 nm. The MCM-41 materials loaded with nanoclusters within their channels have received considerable attention in the past several years, and many nanoclusters have been encapsulated into their channels, such as Ge,[17] Fe_2O_3,[18] GaAs,[19] InP,[20] ruthenium carbonyls,[21] Ru−Ag bimetallic nanoparticles,[22] and GaN.[23] Very recently, we also succeeded in the synthesis of nanosized ZnO[24] in the channels MCM-41 materials by means of a surface modification scheme. The size of the ZnO clusters was found to be <1.8 nm.

ZnS is a semiconductor with a wide band gap and is used commercially as a phosphor and in thin-film electroluminescent devices. ZnS nanocrystals in colloids were recently prepared by Sooklal et al.[25] and Murase et al.[26] Although II−VI semiconductor nanoclusters are currently well investigated because of their many potential applications, there are far fewer studies on ZnS nanoclusters than on CdS and CdSe, which is most likely due to the fact that their bulk band gap is already in the ultraviolet range. In this work, we report our results to illustrate that the mesoporous silica MCM-41 materials can be used as hosts to synthesize nanosized ZnS in their channels by two related schemes, both of which are derived from surface modification of the MCM-41 materials. The MCM-41 sample was first functionalized with ethylenediamine groups, and then Zn^{2+} in ethanol solution was absorbed to form Zn−ED−MCM-41. The resulting sample was directly reacted with H_2S gas or calcined at high temperature to remove the organic component and reacted subsequently with H_2S. In this way, samples of nanozied ZnS inside the MCM-41, with and without organic component, were obtained (designated as ZnS−ED−MCM-41 and ZnS−MCM-41(cal), respectively). The as-prepared ZnS[\]MCM-41 samples were extensively characterized by combined spectroscopic methods. Experimental results show that the ZnS clusters were mostly confined in the channels of the MCM-41 host and the amount of ZnS on the external surfaces is much smaller. A massive blue shift in UV−vis spectra has been observed for the two as-prepared ZnS samples. However, their photoluminescence (PL) properties are very different and possible explanations have been proposed. Finally, we have also explored the preparation of CdS and CuS nanoclusters confined in the channels of the mesoporous hosts.

Experimental Section

Pure siliceous MCM-41 sample was synthesized by the hydrolysis of cetyl trimethylamonium bromide (CTAB) and tetraethyl silicate (TEOS) in basic solution with a final composition of 1.0:7.5:1.8:500 CTAB:TEOS:NaOH:H_2O (mole ratio) and was then treated hydrothermally at 110 °C for 84 h. The mesoporous silica MCM-41 sample was obtained after the parent MCM-41 was calcined at 540 °C for 10 h in air. Functional groups (ethylenediamine groups in this case) were introduced to the pore surfaces of mesoporous silica MCM-41 by refluxing the mixture of calcined MCM-41 and *N*-[3-(trimethoxysilyl)propylethylene]diamine (designated as TPED) (1 g of MCM-41/5 mL of TPED) in dry toluene under a nitrogen atmosphere for at least 10 h. The resulting hybrid materials (ED−MCM-41) are efficient absorbents for Zn^{2+} in water and ethanol solutions. To avoid possible hydrolysis, or even collapse of the siliceous framework in water, Zn^{2+} was absorbed by the ED−MCM-41 in a 0.05 M $Zn(CH_3COO)_2{\cdot}2H_2O$/ethanol solution for about 10 h at room temperature, and the Zn−ED−MCM-41sample was thus obtained. A part of the Zn−ED−MCM-41 sample was calcined at 600 °C in air for 10 h to remove the organic component, giving rise to ZnO clusters in the channels of MCM-41 (ZnO−MCM-41).[24] Finally, the ZnO−MCM-41 samples and another part of the Zn−ED−MCM-41 sample were reacted with H_2S (which was produced by the reaction of $Na_2S{\cdot}9H_2O$ with dilute H_2SO_4) up to 6 h, and ZnS clusters in the channels of MCM-41 (ZnS−MCM-41(cal)) and ED-MCM-41 *(*ZnS−ED−MCM-41) were obtained.

Powder XRD patterns were recorded with a Rigaku Rotaflex diffractometer equipped with a rotating anode, using Cu Kα radiation over the range of $1.8° \leq 2\theta \leq 70°$. Si was used as the internal standard. TEM and EDS analyses were performed by using a JEOL 200CX electron microscope operating at 200 kV. N_2 adsorption−desorption isotherms were obtained on a Micromeritics TriStar 3000 at 77 K under continuous adsorption conditions. BET and BJH analyses were used to determine the total specific surface area (S_{BET}) and the pore size distribution. UV−vis diffuse reflectance spectra were measured on a Shimadzu UV-3101 equipped with an integrating sphere, using $BaSO_4$ as the reference. PL spectra were recorded on a Shimadzu RF-5301 PC spectrofluorophotometer at room temperature.

Results and Discussion

Figure 1 shows the XRD patterns for a series of as-prepared MCM-41 samples within the 2θ range of

(12) (a) Kresge, C. T.; Leonowicz, M. E.; Roth, W. J.; Vartuli, J. C.; Beck, J. S. *Nature* **1992**, *359*, 710. (b) Beck, J. S.; Vartuli, J. C.; Roth, W. J.; Leonowicz, M. E.; Kresge, C. T.; Schmitt, K. D.; Chu, C. T.−W.; Olson, D. H.; Sheppard, E. W.; McCullen, S. B.; Higgins, J. B.; Schlenker, J. L. *J. Am. Chem. Soc.* **1992**, *114*, 10834.

(13) (a) Monnier, A.; Scxhuth, F.; Huo, Q.; Kumar, D.; Margolesse, D.; Maxwell, R. S.; Stucky, G. D.; Krishnamurty, M.; Petroff, P.; Firouzi, A.; Janicke, M.; Chmelka, B. F. *Science* **1993**, *261*, 1299. (b) Firouzi, A.; Kumar, D.; Bull, L. M.; Besier, T.; Sieger, P.; Huo, Q.; Walker, S. A.; Zasadzinsky, J. A.; Glinka, C.; Nicol, J.; Margolesse, D.; Stucky, G. D.; Chmelka, B. F. *Science* **1995**, *267*, 1138−1143. (c) Davis, M. E.; Chen, C.-Y.; Burkett, S.; Lobo, R. *Mater. Res. Soc. Symp. Proc.* **1994**, *346*, 831−842.

(14) (a) Koyano, K. A.; Tatsumi, T.; Tanaka, Y.; Nakzta, S. *J. Phys. Chem. B* **1997**, *101*, 9436. (b) Zhao, X. S.; Lu, G. Q. *J. Phys. Chem. B* **1998**, *102*, 1556. (c) Jaroniec, C. P.; Kruk, M.; Jaronic, M.; Sayari, A. *J. Phys. Chem. B* **1998**, 102, 5503. (d) Feng, X.; Fryxell, G. E.; Wang, L.-O.; Kim, A. Y.; Liu, J.; Kemner, K. M. *Science* **1997**, *276*, 923.

(15) Recent review can be seen: Moller, K.; Bein, T. *Chem. Mater.* **1998**, *10*, 2950.

(16) (a) Fröba, M.; Köhn, R.; Bouffraud, G.; Richard, O.; van Tendeloo, G. *Chem. Mater.* **1999**, *11*, 2858. (b) Luan, Z.; Maes, E. M.; van der Heide, P. A. W.; Zhao, D.; Czernuszewicz, R. S.; Kevan, L. *Chem. Mater.* **1999**, *11*, 3680.

(17) Leon, R.; Margolese, D.; Stucky, G. D.; Petroff, P. M. *Phys. Rev. B* **1995**, *52*, 2285.

(18) Abe, T.; Tachibana, Y.; Uematsu, T.; Iwamoto, M. *Chem. Commun.* **1995**, 1617.

(19) Srdanov, V. I.; Alxneit, I.; Stucky, G. D.; Reaves, C. M.; DenBaars, S. P. *J. Phys. Chem. B* **1998**, *102*, 3341.

(20) Agger, J. R.; Anderson, M. W.; Pemble, M. E.; Terasaki, O.; Nozue, Y. *J. Phys. Chem. B* **1998**, *102*, 2345.

(21) Zhou, W.; Thomas, J. M.; Shephard, D. S.; Johnson, B. F. G.; Ozkaya, D.; Masch-meyer, T.; Bell, R. G.; Ge, Q. *Science* **1998**, *280*, 705.

(22) Shephard, D. S.; Maschmeyer, T.; Johnson, B. F. G.; Thomas, J. M.; Sankar, G.; Ozkaya, D.; Zhou, W.; Oldroyd, R. D.; Bell, R. G. *Angew. Chem., Int. Ed. Engl.* **1997**, *36*, 2242.

(23) Winkler, H.; Birkner, A.; hagen, V.; Wolf, I.; Schmechel, R.; Seggern, H. V.; Fischer, R. A. *Adv. Mater.* **1999**, *11*, 1444.

(24) Zhang, W.-H.; Shi, J.-L.; Wang, L.-Z.; Yan, D.-S. *Chem. Mater.* **2000**, *12*, 1408.

(25) Sooklal, K.; Cullum, B. S.; Angel, S. M.; Murphy, C. J. *J. Phys. Chem.* **1996**, *100*, 4551.

(26) Murase, N.; Jagannathan, R.; Kanematsu, Y.; Watanabe, M.; Kurita, A.; Hirata, K.; Yazawa, T.; Kushida, T. *J. Phys. Chem. B* **1999**, *103*, 754.

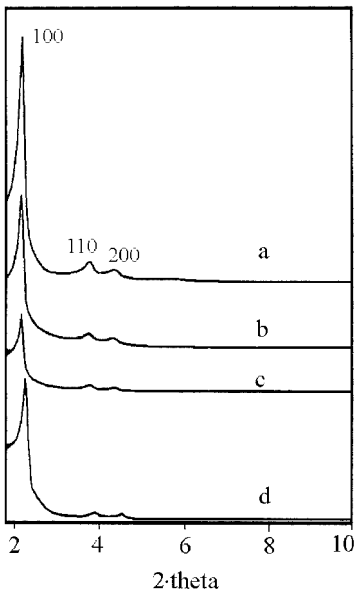

Figure 1. XRD patterns of the series of MCM-41 samples at low angle ranges: (a) calcined MCM-41, (b) ED−MCM-41, (c) ZnS−ED−MCM-41, and (d) ZnS−MCM-41 (cal).

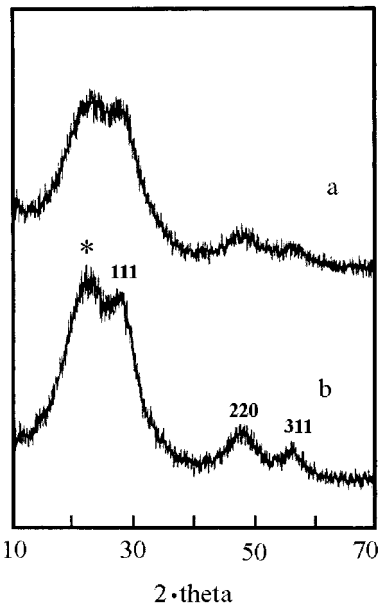

Figure 2. XRD patterns of the as-prepared ZnS/MCM-41 samples at wide angle ranges: (a) ZnS−ED−MCM-41 and (b) ZnS−MCM-41(cal). * is the diffuse peak of noncrystalline silica.

1.8°−10°, all of which display three reflection peaks of typical MCM-41 materials, which shows that MCM-41 materials of high quality were obtained and that hexagonal order was maintained during the formation process of the ZnS clusters. The existence of the ZnS led to a relatively large decrease in the intensities of the characteristic peaks of the MCM-41 materials. This should be attributed to the pore-filling effects that can reduce the scattering contrast between the pores and the framework of the MCM-41 materials. Similar results have been reported previously.[23,24,27] The decrease of the peak intensities of the ZnS−ED−MCM-41 sample is much greater than that of the ZnS−MCM-41(cal) sample, which may be due to the fact that the organic component can also decrease the intensity of the XRD patterns (Figure 1b). Additionally, compared with the d_{100} value of the calcined MCM-41 sample, a slight increase in that of ZnS−ED−MCM-41 and a small decrease in that of ZnS−MCM-41(cal) were found (see Table 1). The reason may be that the filling of the ED groups and the ZnS in the channels of the MCM-41 hosts results in a small increase of the channel period of the ED−MCM-41 and ZnS[\]MCM-41 samples, as reported in ref 20. However, calcination of the Zn−ED−MCM-41 sample at high temperatures results very likely in a framework shrinkage of the MCM-41 material. The latter effect surpasses the filling effect, so that a slight decrease in the lattice of the ZnS−MCM-41(cal) sample was observed.

Figure 2 shows the XRD patterns of the two as-synthesized ZnS[\]MCM-41 samples within the 2θ range of 10°−70°. The three broadened peaks can be attributed to (111), (220), and (311) lattice planes of sphalerite ZnS.[26] The size of the ZnS crystallites was estimated to be <2.5 nm according to the Scherrer formula and compared with the results of ZnO−MCM-41 sample, which were produced in a similar scheme and the size is smaller than 1.8 nm.[24] It is well-known that the large surface area of MCM-41 materials is attributed to the pore system, while only a very small part is provided by the external surfaces. Therefore, the functionalizing reaction and the formation of ZnS clusters should mostly occur in the pore system, and the amount on the external surfaces is much smaller. Specifically, nanosized materials are very easy to sinter when they are thermally treated unless some measures are imposed to stop their growth. In the present experiment, the channels should play such a role in limiting the ZnS growth if it is located inside the channels. However, the ZnS clusters on the external surfaces should grow freely, even into large particles under appropriate conditions. To test this inference, we have annealed the two as-prepared ZnS[\]MCM-41 samples at 150 °C up to 7.5 h under vacuum. However, no changes in the XRD patterns have been detected (not shown), which implies that the nanosized ZnS materials have not grown into large particles. It is possible that the content of the ZnS is too low, thus restraining them from growing. However, chemical analysis shows that the ZnS content is 8.99 and 10.89 wt % for ZnS−ED−MCM-41 and ZnS−MCM-41(cal) samples, respectively. Therefore, we believe that it is the channels of the MCM-41 that have restrained the ZnS growth. The conclusion that most of the ZnS should be located in the channels of the MCM-41 host thus follows. Although there are some ZnS clusters on the external surfaces, the amount is so little that ZnS cannot grow into large particles.

The transmission electron microscopy (TEM) images of the ZnS−MCM-41(cal) sample are shown in Figure 3. Both of the micrographs taken with the electron beam direction parallel to and perpendicular to the channel direction show only the characteristics of MCM-41 materials, and no indication of the ZnS clusters on the external surfaces were observed. However, we still failed to observe directly the existence of ZnS in the channels of the MCM-41 by the TEM method. This is probably due to a weak contrast between the silica frameworks

(27) Mark, B.; Oberhagermann, U.; Vortmann, S.; Gies, H. *Microporous Mater.* **1996**, *6*, 375.

Table 1. Physical Parameters of the Series of As-Prepared MCM-41 Samples[a]

samples	Zn content (wt %)	S content (wt %)	Zn:S (mole ratio)	d_{100} (Å)	surface area (m^2/g)	pore diameter (Å)	pore volume (mL/g)	Si:ED:Zn[a] (mole ratio)
MCM-41				40.13	929.1	28.8	0.776	
ED−MCM-41				40.23	601.4	22.1	0.378	
ZnS−ED−MCM-41	6.09	2.90	1:0.967	40.27	203.3	16.9	0.120	95.5:1:0.704
ZnS−MCM-41(cal)	7.36	3.53	1:0.973	39.05	560.7	21.3	0.319	

[a] ED = 2N.

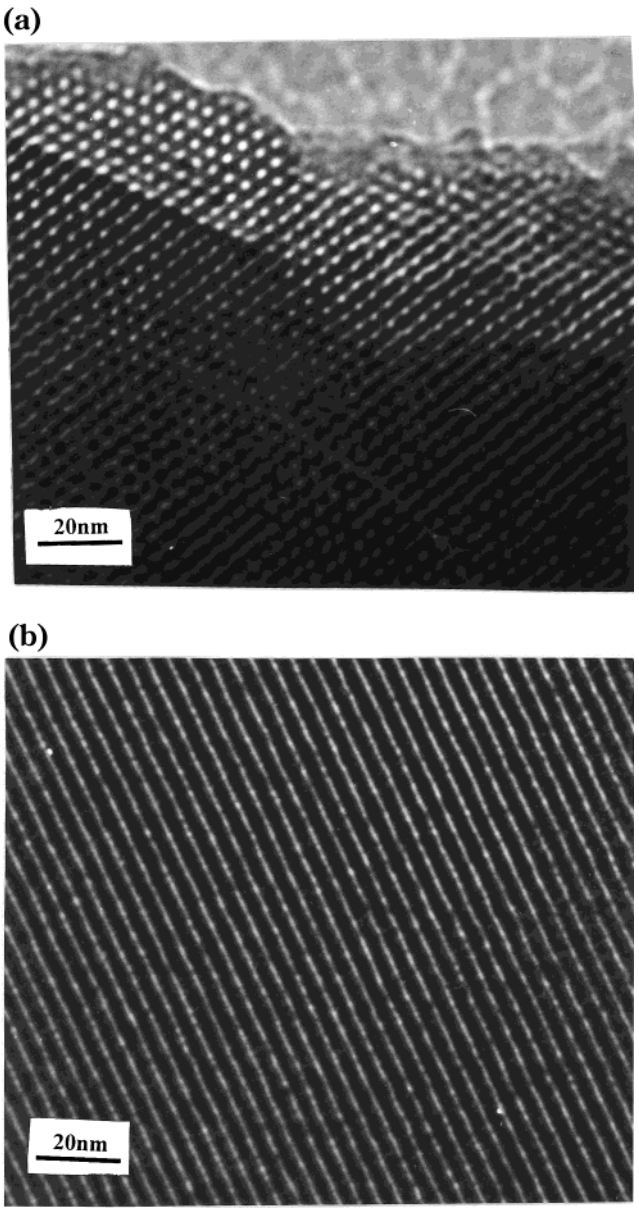

Figure 3. TEM images of the ZnS−MCM-41(cal) sample: (a) micrograph taken with the beam direction parallel to the pore and (b) micrograph taken with the beam direction perpendicular to the pore.

and the nanosized ZnS, as in the case of Fe_2O_3,[18] GaN,[23] and ZnO[24] inside mesoporous hosts. To prove the existence of ZnS inside MCM-41 materials, EDS analysis was made, which showed strong Zn and S signals with an approximate Si:Zn:S atomic ratio of 10.4:1.2:1.0 when the ZnO−MCM-41 sample was reacted with H_2S for 1.5 h, as shown in Figure 4 for the ZnS−MCM-41(cal) sample. The deviation of the Zn:S ratio from 1:1 implied that the reaction between Zn^{2+} and H_2S was

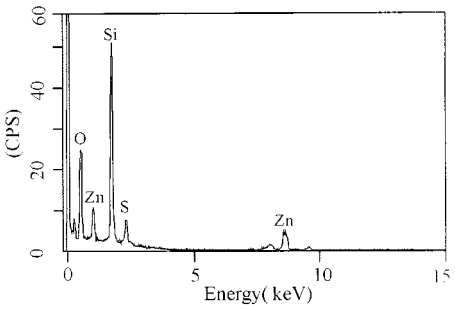

Figure 4. EDS spectrum of the ZnS−MCM-41(cal) sample.

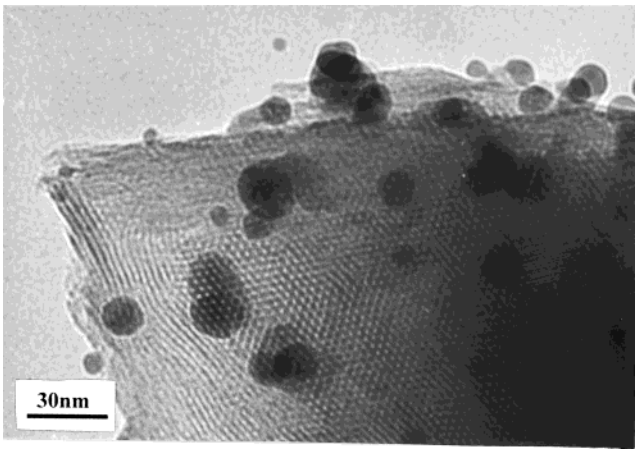

Figure 5. TEM image of the leached ZnS−ED−MCM-41 sample. The sample was stirred in ethanol for 10 min.

not fully complete. However, when the reaction time was extended up to 6 h, the atomic ratio of Zn:S became close to 1:1, despite the fact that elemental S is still a little off stoichiometry (chemical analysis result, see Table 1), which indicates that a long reaction time (between Zn^{2+} and H_2S gas) is an important factor in obtaining pure ZnS in the present scheme. In addition, the TEM images and EDS analyses for the ZnS−ED−MCM-41 sample are essentially the same as those discussed above, so the analysis results for the ZnS−ED−MCM-41 sample are omitted here. These results directly prove that the regularity of the MCM-41 host was maintained during the formation process of the nanosized ZnS, which should be mainly confined in the channels of the MCM-41 host. Finally, the ZnS clusters could be leached out of the channels of MCM-41 and grow into many very large particles on the external surfaces if the ZnS-containing samples were stirred in water or ethanol for more than 4 h. Moreover, this phenomenon is more serious for the ZnS−MCM-41(cal) sample than for the ZnS−ED−MCM-41 sample. Figure 5 gives the TEM image of the ZnS−ED−MCM-41 sample that has been stirred in ethanol for only 10 min. ZnS particles of size much larger than the channel diameter of the MCM-41

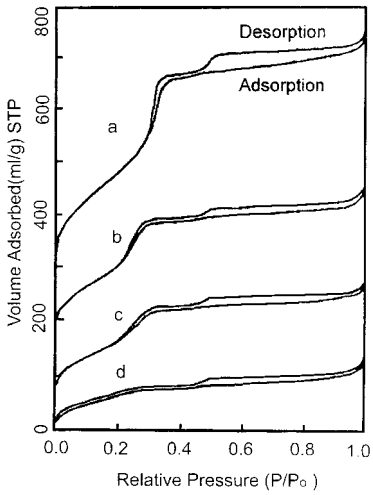

Figure 6. Nitrogen adsorption−desorption isotherms of the series of MCM-41 samples: (a) calcined MCM-41, (b) ED−MCM-41, (c) ZnS−MCM-41(cal), and (d) ZnS−ED−MCM-41.

host were found on the external surface of the mesoporous support. The above results show that the ZnS clusters may only be loosely attached onto the internal surfaces of the MCM-41 hosts and the interaction between the ZnS and the organic groups in the ZnS−ED−MCM-41 sample should be stronger than that between the ZnS and the siliceous framework in the ZnS−MCM-41(cal) sample.

Figure 6 shows the N_2 adsorption−desorption properties of the calcined MCM-41, ED−MCM-41, ZnS−MCM-41(cal), and ZnS−ED−MCM-41 samples. The parameters are also listed in -Table 1. Considerable decreases in the BET surface areas and average pore diameters and pore volumes for the two as-synthesized ZnS[\]MCM-41 samples further indicate that most of the ZnS clusters should be formed and retained in the channels of the MCM-41 hosts. Because of the similarity between the isotherms of samples a, b, and c (MCM-41, ED−MCM-41, and ZnS−MCM-41(cal), respectively) in the present experiment and those of ZnO clusters inside MCM-41 samples,[24] a detailed discussion of these data has been omitted from this paper. Nevertheless, it should be noted that the hysteresis in the high-pressure range (at the relative pressure $P/P_0 \sim 0.45$) should be attributed to the interparticle pores. Very recently, Kruk et al.[28] reported a detailed study on this unusual hysteresis for the MCM-41 materials prepared by using CTAB as the template, and they believed that the secondary mesoporosity is related to the structure of the MCM-41 particles rather than impurities, such as, presumably, layered structures.[29] The isotherm for the ZnS−MCM-41(cal) sample was similar in shape to the calcined MCM-41 sample, which indicates that the ZnS clusters should be dispersed throughout the pores. The mesoporous channels are still accessible, even after the formation of ZnS clusters inside MCM-41 hosts. However, the surface area, pore diameter, and pore volume for the ZnS−ED−MCM-41 sample are significantly smaller in comparison with those of the other three

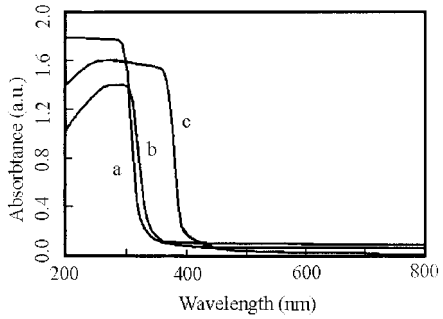

Figure 7. Diffuse-reflectance UV−vis spectra of ZnS-containing samples: (a) ZnS−ED−MCM-41, (b) ZnS−MCM-41(cal), and (c) ZnS bulk.

samples. The isotherm hysteresis for the ZnS−ED−MCM-41 sample extends to very low pressure, which may arise from the irreversible uptake of N_2 in pore structures. These results should mean that the pores of the ZnS−ED−MCM-41 sample may have been partially clogged by the ZnS clusters inside the already narrowed channels of the ED−MCM-41 host.[30] Because of the possible interaction between the ZnS clusters and the organic component of the ZnS−ED−MCM-41 sample, the interfaces between the ZnS clusters and the organic component may have an important contribution to the hysteresis in the N_2 absorption. This interaction also induces a difficulty for the ZnS clusters to be leached out of the channels in comparison with the ZnS−MCM-41(cal) sample when they were stirred in water or in ethanol. To sum up the findings from the XRD patterns, TEM images, EDS analysis, and N_2 physisoption, the nanosized ZnS should mainly be formed and located in the channels of MCM-41, while a relatively small amount of ZnS exists on the external surfaces. The ZnS clusters in the ZnS−MCM-41(cal) sample may form extremely thin films that stick loosely onto the inner walls of the MCM-41. However, the ZnS clusters inside the ZnS−ED−MCM-41 sample should interact with the organic component, inducing a stronger interaction than that between the ZnS and the siliceous frameworks in the ZnS−MCM-41(cal) sample. The ZnS inside the ZnS−ED−MCM-41 sample may also partially clog the channels in some places.

UV−vis diffuse reflectance spectra were used to characterize the absorption properties for the as-prepared ZnS[\]MCM-41 samples, and the spectra are shown in Figure 7. For comparison purposes, the absorption spectrum of bulk ZnS is also given in Figure 7(c). Pure siliceous MCM-41 gives very little absorption in this range.[18] However, the two as-prepared ZnS samples show strong absorption, and both of them show an onset of absorption at ≈350 nm, which is shifted about 60 nm to a shorter wavelength as compared to that of large ZnS particles. The steep absorption edge for the ZnS−ED−MCM-41 sample shifts again 10−20 nm to a shorter wavelength in comparison with that of the ZnS−MCM-41(cal) sample. It should be noted that the results of the present experiment are somewhat different from those of previous work with respect to the absorption edges.[25,26] Considering the fact that the

(28) Kruk, M.; Jaroniec M.; Sakamoto, Y.; Terasaki, O.; Ryoo, R.; Ko, C. H., *J. Phys. Chem. B* **2000**, *104*, 292.

(29) (a) Alfredsson, V.; Keung, M.; Monnier, A.; Stucky, G. D.; Unger, K.; Schuth, F. *J. Chem. Soc., Chem. Commun.* **1994**, 921. (b) Chenite, A.; Le Page, Y.; Sayari, a. *Chem. Mater.* **1995**, *7*, 1015.

(30) Sing, K. S. W.; Everrett, D. H.; Haul, R. A. W.; Moscou, L.; Pierotti, R. A.; Rouquérol, J.; Siemieniewska, T. *Pure Appl. Chem.* **1985**, *57*, 603.

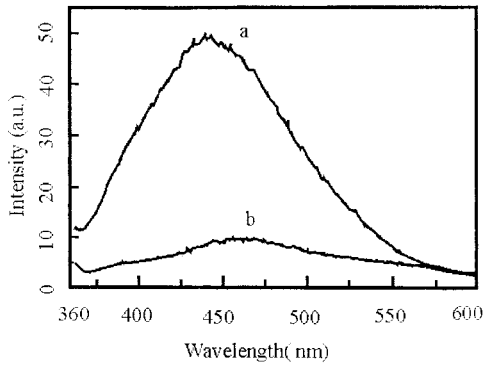

Figure 8. PL spectra of the two as-prepared ZnS[\]MCM-41 samples: (a) ZnS−ED−MCM-41 and (b) ZnS−MCM-41(cal).

optical experiment was performed under identical conditions in the present experiment, the trend of shifting to shorter wavelengths for the absorption edge should reflect the size quantization effect. The organic component in the ZnS−ED−MCM-41 sample diminishes the pore diameters, so that the ZnS clusters can only grow to smaller sizes in comparison with those in the ZnS−MCM-41(cal) system. We have noticed that the shapes of the absorption spectra are very similar for the ZnS−MCM-41(cal) and ZnS bulk, and they are also similar to that of the ZnS inside the pores of a zeolite support, which was prepared by a topotactic MOCVD method and showed dramatic size quantization effects.[31] However, the shape of the absorption spectrum of the ZnS−ED−MCM-41 sample is apparently different. It is well-known that pure siliceous silica is an inert support for many catalysts, such as metals, and metal oxides. The siliceous frameworks of the MCM-41 in the ZnS−MCM-41(cal) sample may pose relatively weak effects on the properties of the ZnS clusters in its channels, so we obtained spectra of very similar shape for the ZnS−MCM-41(cal) and the bulk ZnS samples. However, the organic component may act with the ZnS in the ZnS−ED−MCM-41 sample, which may pose a relatively strong effect on the optical properties, and induce the observed difference from the two former samples in the spectrum shapes. These results show that a relatively strong host−guest effect should exist in the ZnS−ED−MCM-41 sample and a relatively mild effect in the ZnS−MCM-41(cal) composite.

Figure 8 gives the PL spectra of the two as-prepared ZnS[\]MCM-41 samples. Both of them show emissions in the blue range between ≈430 and ≈450 nm. The PL emission of the ZnS−ED−MCM-41 sample shifts about 20 nm to a shorter wavelength in comparison with that of the ZnS−MCM-41(cal) sample, which could arise from the size quantization effect. It must be noticed that the PL intensity of the ZnS−ED−MCM-41 sample is much stronger than that of the ZnS−MCM-41(cal) sample. Dannhauser et al.[32] reported that $N(C_2H_5)_3$ can act as a donor to lower dramatically the nonradioactive decay in CdS and Cd_3As_3 colloids, so as to greatly enhance the PL intensity. Because the chemical properties of ethylenediamine groups are similar to those of $N(C_2H_5)_3$, both of which are Lewis bases, the ED groups may also act as donors to reduce the nonradioactive decay of the ZnS clusters in the present experiment, thus enhancing dramatically the PL intensity, as $N(C_2H_5)_3$ does in the CdS and Cd_3As_2 colloids. In addition, the interfaces induced from the interaction between the ZnS clusters and the organic component may possess a lot of defects in the ZnS−ED−MCM-41 sample. In contrast, the number of defects should be much less in the ZnS−MCM-41(cal) composite because the above-mentioned interfaces should not have existed. Therefore, a considerable enhancement of the PL intensity for the ZnS−ED−MCM-41 sample has been observed.

Up to now, the origin of the blue emission of ZnS has been controversial. Kasaii et al.[33] reported that both Zn^{2+} vacancies and S^{2-} vacancies emitted in the blue ranges between 430 and 450 nm for a self-activated bulk sample. Uchida[34] studied the PL properties of bulk samples in correlation with the off-stoichiometry of Zn and S. He also concluded that samples with both excess Zn and S emitted in the blue range. However, a 395-nm emission has been observed in the Zn excess sample and this emission was assigned to S vacancies. Very recently, Sooklal et al.[25] prepared ZnS nanoclusters with excess Zn in colloids, and blue emission at about 440 nm was observed, which was attributed to sulfur vacancies. In their experiment, EPR (electronic paramagnetic resonance) measurement did not obtain reproducible signals. However, Murase et al.[26] studied the fluorescence and the EPR characteristics of Mn^{2+}-doped ZnS nanocrystals having a mean size of about 4 nm, which were also prepared in colloids. The EPR measurement proved the existence of hole centers such as Zn^{2+} vacancies and they attributed the blue emission at ≈450 nm to the Zn^{2+} vacancy. Therefore, we attribute tentatively the blue emission in the present experiments to the defects related to sulfur vacancies, which is consistent with the result of chemical analysis of the contents of S and Zn. However, the nature of the emission should be further studied to refine the results.

Finally, we have attempted to prepare other sulfide semiconductors inside mesoporous materials by the above schemes. Nanosized CdS inside ED−MCM-41 hosts (CdS−ED−MCM-41) could also be conveniently prepared with good results. However, it is difficult to obtain CdS in the channels of the MCM-41 host without the organic component (CdS−MCM-41(cal)), although some samples with good results were occasionally obtained. Optical experiments also showed that the CdS−ED−MCM-41 sample gave a much stronger PL intensity than the CdS−MCM-41(cal) sample (not shown), which is very similar to the results in the ZnS[\]MCM-41 composites. This proves further that the organic component should pose an important effect on the optical properties of the semiconductors in the channels of the mesoporous hosts. In addition, only a small amount of CuS could be obtained inside the ED−MCM-41 host, which may be mainly due to the high stability of Cu(II)−ED complexes. The Cu−ED−MCM-41 sample could be reacted completely with Na_2S in aqueous solution; however, many large CuS particles have been found on the external surfaces of the MCM-41 materials in the TEM images. Therefore, it can be

(31) Ozin, G. Z.; Steele, M. R.; Holmes, A. J. *Chem. Mater.* **1994**, *6*, 999.
(32) Dannhauser, T.; O'Neil, M.; Johansson, K.; Whitten, D.; McLendon, G. *J. Phys. Chem.* **1986**, *90*, 6047.
(33) Kasai, P. H.; Otomo, Y. *J. Phys. Chem.* **1962**, *87*, 4888.
(34) Uchida, I. *J. Phys. Soc. Jpn.* **1964**, *19*, 670.

expected that the present schemes for preparing sulfide nanoclusters in the channels of the MCM-41 hosts are suitable for preparing materials that can be formed by reacting with gas, but not with anions in solutions. Experiments on other systems are in progress.

Conclusion

The present experiment shows that ZnS nanoclusters have been synthesized in the channels of MCM-41 materials by using two related schemes derived from surface modification methods. The products have been extensively characterized by combined spectroscopic methods, which showed that the ZnS clusters are mostly confined in the channels of the MCM-41. The large blue shift in the absorption spectra for the ZnS[\]MCM-41 samples have been attributed to the size quantization effects. The massive increase of the PL intensity for ZnS−ED−MCM-41 sample is believed to be due to the strong interaction between the ZnS clusters and ethylenediamine groups. A strong host−guest effect for ZnS−ED−MCM-41 and a weak effect for ZnS−MCM-41(cal) materials were suggested.

The successful syntheses of ZnS and other sulfides inside the mesoporous silica MCM-41 confirm the variability of the MCM-41 materials as hosts for encapsulating guest materials. Surface modification via a chemical route may have significant advantages over direct synthesis methods (e.g., ion exchange and MOCVD schemes) in fabricating organized composites with desirable properties. Specific groups in the functionalized monolayers have been used to attach new functional groups[35] or to stimulate mineral deposition.[36] We believe that the ordered mesoporous materials modified by functional groups will play a significant role in host−guest chemistry development.

Acknowledgment. This work was supported by the National Natural Science Foundation of China, Grant 59882007.

CM000621R

(35) Fryxell, G. E.; Rieke, P. C.; Wood, L. L.; Engelhard, M. H.; Williford, R. E.; Graff, G. L.; Campbell, A. A.; Wiacek, L. L.; Halverson, A. *Langmuir* **1996**, *12*, 5064.
(36) Calvert, P. *Nature* **1988**, *334*, 651.